CONCEPT DEVELOPMENT AND PREDICTION OF VCR ENGINE PERFORMANCE USING SLIDER CRANK PIN MECHANISM BASED ON QUASI-DIMENSIONAL COMBUSTION MODELING

by

Jeewan Vachan TIRKEY*

Department of Mechanical Engineering, Indian Institute of Technology (BHU), Varanasi, India

Original scientific paper
https://doi.org/10.2298/TSCI170518296T

Energy, economy and pollution factor of internal combustion engine profoundly influence the development of the society. It is well known that efficiency of an internal combustion engine increases by compression ratio, and is limited due to knocking and high thermal stress development in the combustion chamber of an engine. On another side, an efficiency of internal combustion engine decreases toward the more top engine speed. Considering this, a concept is proposed which can change its compression ratio with speed. Variation in compression ratio is achieved by a change in stroke length through moving crank pin within the crank. In this paper the mechanism of operation and prediction of performance characteristics of variable compression ratio spark ignition engine with varying speed using quasi-dimensional combustion simulation mode is presented. It was observed that proposed mechanism provides better fuel efficiency at higher engine speed. Further, it is inferred that 3 mm increase in crank length results in 7% increment in thermal efficiency and 8% decrement in brake specific fuel consumption for 13 compression ratio at 6000 rpm.

Key words: *simulation, variable compression ratio, engine speed, efficiency, slider crank pin, spring stiffness, brake specific fuel consumption*

Introduction

Growing energy demand and strict emission norms have forced to develop more efficient, economical and reduced emission vehicles. The conventional internal combustion (IC) engine operates on the fixed compression ratio (FCR). It is recognized that the indicated fuel conversion efficiency decreases and specific fuel consumption increases with increase in engine speed. Sezer [1] validated the experimental results with a computational model for FCR and showed that the brake thermal efficiency (BTE) decreases and brake specific fuel consumption (BSFC) increases with increasing engine speed from mid-range. On the other hand, Costa and Sodre [2] studied that the power output and specific fuel consumption improve by increasing compression ratio (CR) due to the high pressure produced from combustion. Moreover, higher CR increases fuel-air mixture density and turbulence in the combustion chamber in turn increases cylinder pressure and fast burning speed. However, a few modern internal combustion engine (ICE) have also been reported to work at a fixed compression ratio of 10 to 14:1 for spark ignition (SI) engines and 16:1 to 18:1 for compression ignition (CI) engines [3]. Variable compression ratio (VCR) of an engine can be obtained through either change in clearance volume or stroke volume. Yamin and Dado [4] simulated the variable-stroke engine with an eight-link

* Author's e-mail: jvtirkey@gmail.com

mechanism to provide variable stroke lengths and variable compression ratios and found significant fuel efficiency. The VCR engine is used to achieve high efficiency at a low power level to gain more mileage because automobile operates at low power levels most of the time. Alagumalai [5] reviewed the work of Raheman and Ghadge and reported that BTE of Mauha bio-diesel fueled Diesel engine increases by 29.5% by varying CR from 18:1 to 20:1. Low CR prevents knocking of an engine at high load while high CR at low load, which could be solved by VCR engine. Montoya *et al.* [6] studied the blends of fuel and suggested that reduced equivalence ratio of the fuel-air mixture improves resistance to knocking. The SI VCR engine can provide efficient performance and less emission with gasoline fuel and alternative fuel [7]. Also, the change in CR plays a vide role for the control of combustion duration [8]. Muralidharan *et al.* [9] investigated the impacts of different CR (18-22) on a VCR engine using waste cooking oil methyl esters and diesel blends. The experimental outcomes exhibited a significant increase in BTE and improvement in fuel economy with an increasing CR. Similarly, Hora and Agarwal [10] experimentally analyzed that BTE and BSFC improve with increases in CR corresponding to excess air-fuel ratio of hydrogen-enriched natural gas. However, peak in-cylinder pressure becomes higher. Roberts [11] reviewed several complicated designs of VCR like moving the cylinder head, variation of combustion chamber volume, variation of piston deck height and modification of connecting rod geometry using intermediate member for enhancement of engine performance. Although, some of them have been designed for experimental purpose in the laboratory. Pešić *et al.* [12] investigated the various methods of implementing VCR and its challenges on the performance on Diesel engine.

In addition to, computer simulation plays an important role to investigate performance and feasibility studies with short time, instead of a long time spent in the complicated experimental process. The authors [13-17] used zero and quasi-dimensional combustion model and observed that BTE decreases and BSFC increase with higher engine speed. Also, fuel conversion efficiency increases with increase in CR under the limit of knock. Regarding emission mitigation, Mardi *et al.* [18] showed that CO emission increases towards higher engine speed due to incomplete combustion. Furthermore, the efficiency of the IC engine can be improved by using change in the power cycle. Gonca *et al.* [19], and Gonca [20] suggested that the Miller cycle and Atkinson cycle is efficient and environmentally friendly to the Diesel engines using single zone and two-zone combustion modeling. Dorić and Klinar [21] illustrated the significant reduction in fuel consumption while simulating variable compression ratio engine through movement of piston linked with two pairs of a non-circular gear mechanism.

Although, there are many works have been reported in the literature regarding methods to enhance the efficiency using VCR, the literature on high engine speed and a corresponding change in CR are quite a few. Therefore, a novel concept has been proposed to achieve suitable VCR corresponding to the change in speed. Thus, the objective of the paper is to imply a mechanism to obtain the VCR at higher speed range on the engine, which in turn enhances the performance of a SI engine. For this, modification in the crank with a sliding crank pin has been proposed to change the crank length and corresponds to CR. The required change in the crank length is accomplished by centrifugal force acting on the spring controlled sliding crank pin in the slotted crank, which rotates about the crankshaft axis as well. A computational quasi-dimensional combustion model was applied to analyze the forces acting on the crank and corresponding performance characteristic of SI engine for both FCR and VCR. The simulation result showed a good agreement with the experiment of fixed compression ratio and therefore, prediction of the engine performance. The simulation results also exhibited that proposed concept provides significant improvement in thermal efficiency and low fuel consumption.

Mathematical combustion model

The mathematical model is incorporated into the base of the model taken by different authors [3, 22, and 26]. Assumption and description of quasi-dimensional combustion model are:

- cylinder contains homogeneous mixture of charges during the cyclic processes,
- in two-zone combustion, the effect of thin-film reaction region between burned and unburned zone is negligible,
- the heat transfer between the burned and unburned zones is negligible,
- there is uniform pressure throughout the cylinder at any time,
- thermal properties are calculated using polynomial coefficient of each gas,
- all crevices, blow-by losses are not considered,
- cylinder wall temperature (500 K) is uniform and constant, and
- the burned gasses are in thermodynamic equilibrium except for the N and CO species.

Compression

Compression started from inlet valve close (IVC), and the trapped mixture is of fresh charge and residual species of the previous cycle. It is assumed that during this process no reaction occurs and gas mixture is perfect. The First law of thermodynamics to the cylinder charge and equation of state gives the following relations to calculate pressure and temperature concerning crank angle [27]:

$$\frac{\mathrm{d}p}{\mathrm{d}\alpha} = \left[\frac{R}{C_v}\left(\frac{\mathrm{d}Q}{\mathrm{d}\alpha}\right) - \frac{p\mathrm{d}V}{\mathrm{d}\alpha}\left(\frac{R}{C_v}+1\right)\right]\frac{1}{V} \tag{1}$$

$$\frac{\mathrm{d}T_m}{\mathrm{d}\alpha} = T_m\left(\frac{1}{V}\frac{\mathrm{d}V}{\mathrm{d}\alpha} + \frac{1}{p}\frac{\mathrm{d}p}{\mathrm{d}\alpha}\right) \tag{2}$$

The piston work is given:

$$\frac{\mathrm{d}W}{\mathrm{d}\alpha} = p\frac{\mathrm{d}V}{\mathrm{d}\alpha} \tag{3}$$

The rate of heat transfer from gas to the wall is calculated by Annand's equation [15-17]:

$$\frac{q}{k} = \frac{ak_q\,\mathrm{Re}^b(T_m - T_w)}{D} + c(T_m^4 - T_w^4) \tag{4}$$

where k_q is thermal conductivity, $k_q = (\mu c_p)/0.7$; here a, b, and c are constants, $a = 0.4$, $b = 0.7$, $c = 4.3\cdot10^{-9}$.

As the compression process is continued, the variables are incremented by:

$$X_{n+1} = X_n + \left(\frac{\mathrm{d}X}{\mathrm{d}\alpha}\right)\Delta\alpha \tag{5}$$

where X is any variable. The numerical solution was conducted using fourth-order Runge-Kutta method.

Ignition and initiation of two-zone

After ignition, the compression process is continued over the period of ignition lag. After that, two-zone combustion process starts, where flame kernel spontaneously appears in the cylinder. It is assumed that the flame nucleus formed at constant specific volume combus-

tion causes high pressure and temperature in the products region. The initial value of the product temperature has been guessed by Annand's expression [25]. The assumption of constant volume combustion produces a pressure difference between the burned and unburned zones which is physically impossible; therefore, pressure equalization process is taken into consideration [22]. Combustion propagation is carried out with the speed of the turbulent flame speed.

The laminar flame speed, S_L, is calculated [3]:

$$S_L = S_{us}\left(\frac{T_u}{T_{us}}\right)^{\alpha}\left(\frac{P}{P_{us}}\right)^{\beta} \tag{6}$$

where P_{us} = 0.1 MPa, T_{us} = 300 K are reference pressure and temperature and S_{us}, α, and β are constants for a given fuel, equivalence ratio (Φ), and burned gas diluent fraction. For gasoline, these constants can be presented [3]:

$$S_{us} = 30.9 - 54.9(\Phi - 1.12)^2,\ \alpha = 2.4 - 0.271\ \Phi^{3.51},\ \beta = -0.357 + 0.14\ \Phi^{2.77} \tag{7}$$

There are several empirical relations to describe and calculate the turbulence flame speed, S_T, of gasoline. Klimov's [28] proposed relation has been used to calculate turbulent flame speed:

$$S_T = (u')^{0.7}(S_l)^{0.3} \tag{8}$$

where u' is RMS value of turbulent flame intensity and determined by [25]:

$$u' = 0.57 S_p \frac{1 - 0.5(\theta - 180)}{45} \tag{9}$$

where S_p is mean piston speed and θ is the crank angle (TDC at 180°).

The mass burning rate is determined by [25]:

$$\frac{\mathrm{d}mb}{\mathrm{d}t} = A_f \rho_u S_T \tag{10}$$

where A_f is the flame front area, and it is calculated by the geometrical model. The detail of geometrical model for flame front area propagation is followed by the reference [24].

Expansion with two-zone

The assumptions for this model are:

- the charges are homogeneous,
- the pressure is uniform throughout the cylinder,
- the volume occupied by the flame reaction zone is negligible,
- the burned gases are in thermodynamic equilibrium except for the NO_x, and
- no heat transfer between burned and unburned zones. First law of thermodynamics, energy equation, flame speed, and corresponding geometry of the burned zone with the combustion chamber are used to calculate temperature and pressure of the burned and unburned mixture [22, 25, 27]:

$$\frac{\mathrm{d}Tm}{\mathrm{d}\alpha} = \frac{1}{m_m c_{pm}}\left(V_m \frac{\mathrm{d}p}{\mathrm{d}\alpha} + \frac{\mathrm{d}Q_m}{\mathrm{d}\alpha}\right) \tag{11}$$

$$\frac{\mathrm{d}Tp}{\mathrm{d}\alpha} = \frac{p}{m_p R_p}\left[\frac{\mathrm{d}V}{\mathrm{d}\alpha} - \left(\frac{R_p T_p}{p} - \frac{R_m T_m}{p}\right)\frac{\mathrm{d}m_p}{\mathrm{d}\alpha} - \left(\frac{R_m V_m}{P c_{pm}}\right)\frac{\mathrm{d}p}{\mathrm{d}\alpha} - \left(\frac{R_m}{P c_{pm}}\right)\frac{\mathrm{d}Q_m}{\mathrm{d}\alpha} + \left(\frac{V}{P}\right)\frac{\mathrm{d}p}{\mathrm{d}\alpha}\right] \tag{12}$$

$$\frac{\mathrm{d}p}{\mathrm{d}\alpha}=\frac{\left(1+\frac{c_{v_m}}{R_p}\right)P\frac{\mathrm{d}V}{\mathrm{d}\alpha}+\left[(u_p-u_m)-c_{v_p}\left(T_p-\frac{R_mT_m}{R_p}\right)\right]\frac{\mathrm{d}m_p}{\mathrm{d}\alpha}+\left(\frac{c_{v_m}}{c_{p_m}}-\frac{c_{v_p}}{R_p}\frac{R_m}{c_{p_m}}\right)\frac{\mathrm{d}Q_m}{\mathrm{d}\alpha}-\frac{\mathrm{d}Q}{\mathrm{d}\alpha}}{\frac{c_{v_p}}{c_{p_m}}\frac{R_m}{R_p}V_m-\frac{c_{v_m}}{c_{p_m}}V_m-\frac{c_{v_p}}{R_p}V} \tag{13}$$

The variables are incremented by the Runge-Kutta method and assumed that combustion terminated at the beginning of the time step where the current value of unburned volume tends to negative. Once combustion is completed, the variables are organized for a single-zone calculation.

Working of variable crank mechanism

In the ICE, the piston reciprocates inside the cylinder, and the crank rotates about the crankshaft. It is depicted in fig. 1 that the spring is placed into the slotted groove of the crank. The spring is rigidly connected with two ends. One end is fixed on crank itself and another end with a sliding block. The sliding block is coupled with the big end of connecting rod with crankpin, and the piston is pivoted with the small end of the connecting rod. During the crank revolution, the crank pin is stressed by centrifugal force, which acts radially outward in direction. The centrifugal force of the rotating crank is utilized to slide the spring loaded block (having weight) on a slotted crank. When the engine runs at lower speed, centrifugal force reduces deformation in spring and sliding block. Also, the lesser increment of crank length provides reduced CR. On other side, when the engine runs at higher speed, centrifugal force, $mr\omega^2$, increases with engine rpm which produces more elongation in spring resulting in more sliding of block. This has effect on piston to travel more distance toward TDC through increased crank and connecting rod of cylinder. This causes decrease in clearance volume and hence increase in CR. Thus the variable compression ratio in an engine can be obtained automatically during a change in the engine speed by using spring coupled slider block variable crank length mechanism. The changes in compression ratio can be monitored by using engine endoscope integrated with high-speed camera, or else by observing an increase in cyclic peak pressure using pressure transducer.

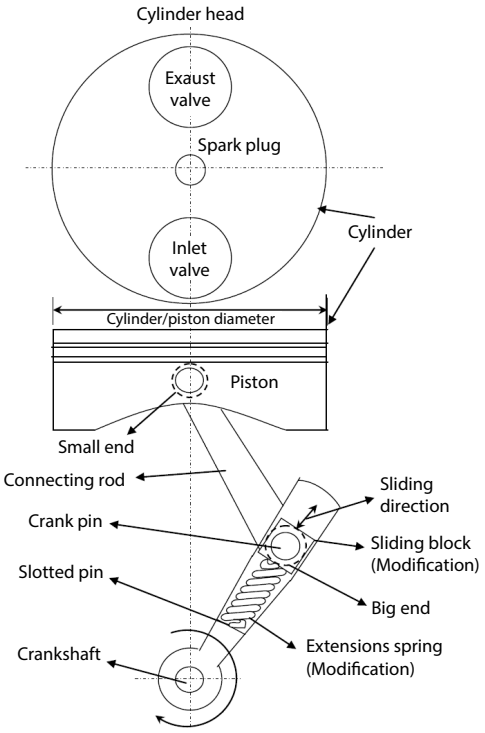

Figure 1. Spring-block slider variable crank length mechanism for VCR engine

Considering safety regarding resistance to gas flow into the engine and material strength against knocking of an engine, the ranges of CR has been fixed from 8-13 for 1000-6000 rpm corresponding to 0.0 to $3.0945\cdot10^{-3}$ m crank length increment required. These ranges can be changed as per different type of reciprocating engine design like SI, CI (12-20 CR), and for alternative fuel.

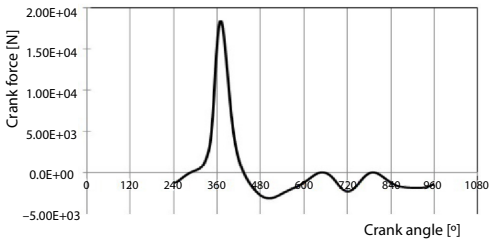

Figure 2. Forces acting on the crank along radial direction *vs.* crank angle (TDC at 360°) at full load

Figure 2 shows the forces acting along the crank at full throttle. The direction of force (inward or outward) varies with angle. The positive sign in the figure represents radially inward force which tends to push slider crank pin inward to achieve lower CR. And the negative sign represents radially outward force corresponding to crank shaft which pulls slider crank pin outward for higher CR. Thus, centrifugal forces generated at slider crank pin with the engine speed changes the effective length of the crank which results in terms of CR variation.

Dynamic analysis of model

During the engine operation, combustion gas pushes the piston; the net force acting on the crank in the radial direction including revolving crank mass at the crank is given:

$$F_{net} = Mr\omega^2 - \left[\frac{\cos(\theta+\phi)}{\cos\phi}\right]\left[pA - mr\omega^2\left(\cos\theta + \frac{\cos 2\theta}{n}\right)\right] \tag{14}$$

where p is cylinder gas pressure, A – the cross-sectional area of the cylinder bore, M – the crank mass, m – the reciprocating mass sliding block, r – the distance between crankshaft and sliding block, and ω is the crank revolution in radian. The change in crank length is calculated:

$$\Delta l = \frac{F_{net}}{k} \tag{15}$$

where k is spring constant.

After the calculation of maximum tension force and required deflection in crank length concerning reciprocating mass and corresponding centrifugal force, the value of spring constant, k, is obtained by trial and error method and is equal to 5·106 Nm corresponding to 1.0 kg crank mass and 0.75 kg reciprocating mass. It is assumed that crank length elongates toward TDC and BDC with centrifugal effect on crank mass. The new stroke length can be calculated by:

$$SL_{\text{new}} = \frac{(CR_{\text{ref}}+1)(CR_{\text{new}}-1)}{(CR_{\text{ref}}-1)(CR_{\text{new}}+1)} SL_{\text{ref}} \tag{16}$$

where SL_{ref} is the reference stroke length corresponding to reference compression ratio CR_{ref}.

Change in crank length, Δl, with respect to reference crank length can be calculated:

$$\Delta l = \frac{SL_{\text{new}} - SL_{\text{ref}}}{2} \tag{17}$$

With respect to eq. (17), fig. 3 shows the variation of CR and corresponding required crank length.

Model Validation

Figure 4 shows the validation of in-cylinder pressure history of simulation and experimental result. The experiment was conducted on a Kirloskar made, single cylinder, 4-stroke, variable speed, water-cooled, cylinder bore 0.0875 m, stroke length 0.110 m, connecting rod length 0.234 m, fixed cr 10.00, swept volume $661.45\cdot10^{-6}$ m^3 and having maximum power 3.50 kW at 1800 rpm. The test engine is coupled with an eddy current dynamometer for mea-

suring speed and load (Make Saj test plant Pvt. Ltd., Model AG10, load accuracy of ±0.1 kg). The cylinder gas pressure is measured with a piezoelectric pressure transducer (Make PCB Piezotronics, Model SM111A22, Range up to 5000 ±2 psi is mounted on the cylinder head. The developed computer simulation program predicts the engine performance, which consists of two-zone combustion, and inlet and exhaust pipe gas dynamics. The prediction of the performance of an SI engine is based on the 4-stroke SI engine as specified in tab. 1. The simulated results reasonably compare with the experimental observations, fig. 4. Deviations between the observed data and simulated results may be attributed to the involved assumptions that consider charges as a homogeneous mixture along with no variability in power cycle.

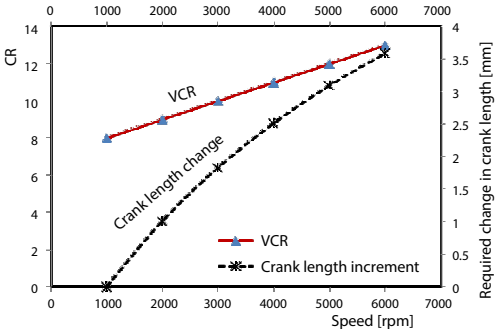

Figure 3. Variation of CR and crank length with speed for VCR engine at full load

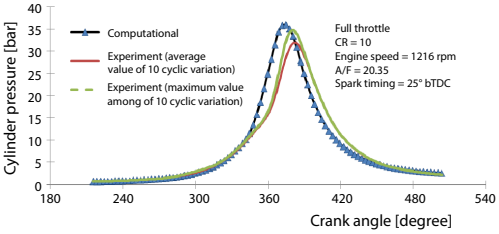

Figure 4. Validation of pressure crank angle at full load

Results and discussion

The simulation of engine performance is considered to be run in full throttle, variable load (or speed) operating condition. At the full throttle, engine provides maximum brake power at one given engine speed. At this speed, it will be carrying a certain load, which if increased, will decrease the speed and thus the brake power [29]. The comparisons of engine performance between fixed compression ratio (FCR = 9.5) and VCR at full throttle are shown in fig. 5. It can be predicted that VCR engine provides more efficiency and more power toward the high engine speed in comparison to FCR. It is evident from the figure that spring slider variable crank length can be used to increase the engine efficiency and decrease fuel consumption. This mechanism can be used to improve performance in the Diesel engine, alternative fuel engine (SI and CI both), and in over expanded engine.

Table 1. The SI engine specification

Gasoline fuel	C_7H_{13}
Equivalence ratio	1.00
Calorific value of fuel, [kJkg^{-1}]	44000.0
Engine revolution, [rpm]	1000-6000.00
Compression ratio (ref)	8.00
Compression ratio (new)	8-13
Cylinder diameter, [m]	0.0953
Stroke length (ref.), [m]	0.0704
Stroke length (new), [m]	0.0704-0.0776
Increase in crank length, [mm]	0.0-3.0945
Connecting rod length, [m]	0 .1365
Exhaust valve open	114.6° (65.4 °bBDC)
Exhaust valve closes	393.4° (33.4 °aTDC)
Inlet valve opens	326.6° (33.40 °bTDC)
Inlet valve closes	605.4° (65.40 °aBDC)
Angle of ignition	686.4° (33.60 °bTDC)
Spark plug position/bore	0.3517
Inlet valve diameter/bore	0.4410
Exhaust valve diameter/bore	0.3990

The indicated power (IP) is the rate of work transfer from gases in the engine cylinder to the piston, and the brake power (BP) is the power at the crank shaft. All IP is not available at the crank shaft (BP), and the difference is due to presence of total friction power. The total friction

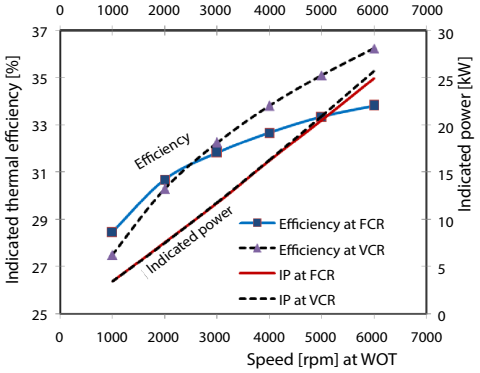

Figure 5. Thermal efficiency and IP at different speed for FCR and VCR engine

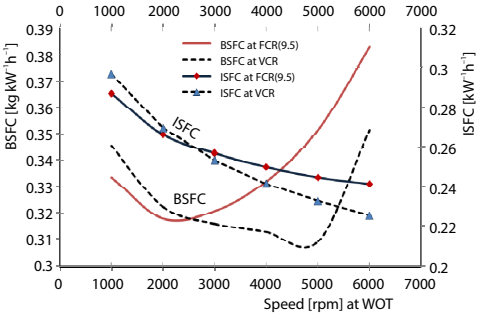

Figure 6. The ISFC and BSFC at different speed for FCR and VCR

mean effective pressure was calculated for friction power through empirical relation [3]. This helps to calculate ISFC corresponding to IP and BSFC corresponding to BP.

Figure 5 also shows that IP of VCR engine is lower than IP of FCR engine at speed less than 3000 rpm. However, the advantage of speed rise beyond 3000 rpm and above has been observed in terms of increase in IP of VCR engine by 0.0057%, 0.3445%, 2.076%, and 3.017% at 3000 rpm, 4000 rpm, 5000 rpm, and 6000 rpm, respectively, when compared with FCR engine. Also, below 3000 rpm speed BTE of VCR is less and beyond 3000 rpm BTE of VCR engine increases by 1.3509%, 3.525%, 5.298%, and 7.1699% at 3000 rpm, 4000 rpm, 5000 rpm, and 6000 rpm, respectively, as compared with FCR engine.

Indicated specific fuel consumption (ISFC) signifies the fuel consumption in an engine. Figure 6 shows that ISFC and BSFC of VCR are significantly reduced from the 2500 rpm to 6000 rpm, in comparison to FCR. However, at speed lower than 2500 rpm, ISFC of VCR engine is increased in comparison with FCR engine. In sum it can be observed that as the speed increases towards 3000 rpm and above, the ISFC of VCR engine decreases by 1.31%, 3.39%, 4.78%, and 6.70% at 3000 rpm, 4000 rpm, 5000 rpm, and 6000 rpm, respectively, when compared with FCR engine. Similarly below 3000 to 2500 rpm speed, BSFC of VCR is less than FCR engine and at more than 3000 rpm the BSFC of VCR engine decreases by 1.44%, 5.74%, 11.98%, and 8.23% at 3000 rpm, 4000 rpm, 5000 rpm, and 6000 rpm, respectively, compared to FCR engine.

Conclusion

In the present study, a computational analysis has been conducted to explore the performance characteristics of the VCR-SI engine and compared with the FCR-SI engine.

By thorough computational investigations, following salient conclusions have been drawn.

- On increasing CR, the combustion is found to be boosted with faster combustion rate and it assists in reduction of residual gases which is one of the essential factors for improvement in thermal efficiency. It was observed that there is a significant improvement in thermal efficiency beyond 2000 engine rpm and goes on increasing up to 7% which corresponds to 6000 engine rpm and 13 CR.
- The IP of VCR increases with increase in speed and corresponding CR. It has also been observed that IP increases 0.4% at engine speed 3000 rpm and goes on increasing up to 3.0 % at engine speed 6000 rpm with 13 CR when compared to 9.5 FCR.
- The BP of VCR engine increases with speed and change in CR. It is intresting to note that BP also increses by 0.7% at engine speed 3000 rpm and goes on increasing by about 4.7% at engine speed of 6000 rpm with 13 CR compared to 9.5 FCR at the same speed.

- Indicated specific fuel consumption decreases with increase in speed and CR. It has been seen that reduction in ISFC started from 3000 rpm and reached 6.7% at engine speed 6000 rpm with 13 CR compared to 9.5 FCR.
- Brake specific fuel consumption decreases corresponding to increase in engine speed and proportional to CR. Further the reduction was observed 1.5% at 3000 rpm and about 8.2% at engine speed 6000 rpm with 13 CR as compared to 9.5 FCR.

Since CR changes with the speed of the engine, a significant improvement in thermal efficiency and saving in fuel consumption can be obtained. Therefore, alternative fuels and its blending with conventional fuel can be applied to the proposed mechanism at higher CR.

Nomenclature

A – bore area, [m^2]
A_s – surface area exposed to heat transfer, [m^2]
a, b – Annand's constant
d – cylinder bore, [m]
h – convection heat transfer coefficient, [Wm^{-2}K^{-1}]
k – spring constant, [Nm^{-1}]
Δl – elongation of the spring, [mm]
l – connecting rod length, [m]
m – mass, [kg]
m_a – mass of air, [kg]
m_f – mass of fuel, [kg]
N – engine speed, [rpm]
n – ratio of connecting rod length to crank length
P_{us} – reference pressure
p – mean piston speed, [ms^{-1}]
R – characteristic gas constant [kJkg^{-1}K^{-1}]
S_L – laminar flame speed
S_T – turbulent flame speed
T_{us} – reference temperature
T_m – mean burn temperature
V – cylinder volume, [m^3]
V_c – clearance volume, [m^3]
V_s – swept volume, [m^3]

Greek symbols

ω – angular velocity, [rad s^{-1}]
γ – ratio of specific heats
θ – deg. crank angle,
θ_d – duration of heat release, deg. crank angle
θ_s – spark timing, deg. crank angle
Φ – equivalence ratio

Subscripts

a – air
c – clearance
f – fuel
m – mean
L – laminar
T – turbulent

Acronyms

BTE – brake thermal efficiency
BSFC – brake specific fuel consumption
CI – compression ignition engine
CR – compression ratio
FCR – fixed compression ratio
ICE – internal combustion engine
ISFC – indicated specific fuel consumption
SFC – specific fuel consumption, [gkW^{-1}h^{-1}]
SI – spark ignition engine
VCR – variable compression ratio

References

[1] Sezer, I., Thermodynamic, Performance and Emission Investigation of a Diesel Engine Running on Dimethyl Ether and Diethyl Ether, *International Journal of Thermal Sciences, 50* (2011), 8, pp. 1594-1603
[2] Costa, R. C., Sodre, J. R., Compression Ratio Effects on an Ethanol/Gasoline Fuelled Engine Performance*, Applied Thermal Engineering, 31* (2011), 2-3, pp. 278-283
[3] Heywood, J. B., *Internal Combustion Engine Fundamental*, McGraw-Hill, Inc., New York, USA, 1988
[4] Yamin, J. A. A., Dado, M. H., Performance Simulation of a Four-Stroke Engine with Variable Stroke-Length and Compression Ratio, *Applied Energy, 77* (2004), 4, pp. 447-463
[5] Alagumalai, A., Internal Combustion Engines: Progress and prospects, *Renewable and Sustainable Energy Reviews, 38* (2014), C, pp. 561-571
[6] Montoya, J. P. G., *et al*., Prediction and Measurement of the Critical Compression Ratio and Methane Number for Blends of Biogas with Methane, Propane and Hydrogen, *Fuel, 186* (2016), Dec., pp. 168-175
[7] Balki, M. K., Sayin, C., The Effect of Compression Ratio on the Performance, Emissions and Combustion of an SI (Spark Ignition) Engine Fueled with Pure Ethanol, Ethanol and Unleaded Gasoline, *Energy, 71* (2014), C, pp. 194-201

[8] Bayrakar, H., Durgun, O., Development of an Empirical Correlation for Combustion Durations in Spark Ignition Engines, *Energy Conversion and Management, 45* (2004), 9-10, pp. 1419-1431
[9] Muralidharan, K., *et al.,* Emission and Combustion Characteristics of a Variable Compression Ratio Engine Using Methyl Esters of Waste Cooking Oil and Diesel Blends, *Applied Energy, 88* (2011), 11, pp. 3959-3968
[10] Tadveer, S. H., Kumar, A. A., Effect of Varying Compression Ratio on Combustion, Performance, and Emissions of a Hydrogen Enriched Compressed Natural Gas Fuelled Engine, *Journal of Natural Gas Science and Engineering, 31* (2016), Apr., pp. 819-828
[11] Roberts, M., Benefits and Challenges of Variable Compression Ratio (VCR), SAE International, Apr., 2003-01-0398, 2003
[12] Pešić, B. R., *et al*., Benefits and Challenges of Variable Compression Ratio Diesel Engine, *Thermal Science*, *14* (2010) 4, pp. 1063-1073
[13] Ramachandran, S., Rapid Thermodynamic Simulation Model of an Internal Combustion Engine on Alternate Fuels, *Proceeding*, International Multi Conference of Engineers and Computer Scientists, Hong Kong, China, Vol. 2, 2009
[14] Al-Baghdadi, M., Sadiq, A. R., A Simulation Model for a Single Cylinder Four-Stroke Spark Ignition Engine Fueled with Alternative Fuels, *Turkish J. Eng. Env. Sci., 30* (2006), pp. 331-350
[15] Chaudharia, A. J., *et al*., Simulation Models for Spark Ignition Engine: A Comparative Performance Study, *Energy Procedia, 54* (2014), Dec., pp. 330-341
[16] Ramadhas, A. S., *et al*., Theoretical Modeling and Experimental Studies on Biodiesel-Fueled Engine, *Renewable Energy, 31* (2006), 11, pp. 1813-1826
[17] Liu, S., *et al*., Study of Spark Ignition Engine Fueled with Methanol/Gasoline Fuel Blends, *Applied Thermal Engineering, 27* (2007), 11-12, pp. 1904-1910
[18] Mardi, M. K., *et al.*, A Numerical Investigation on the Influence of EGR in a Supercharged SI Engine Fueled with Gasoline and Alternative Fuels, *Energy Conversion and Management, 83* (2014), July, pp. 260-269
[19] Gonca, G., *et al.,* Theoretical and Experimental Investigation of the Miller Cycle Diesel Engine in Terms of Performance and Emission Parameters, *Applied Energy, 138* (2015), Jan., pp. 11-20
[20] Gonca, G., Performance Analysis and Optimization of Irreversible Dual-Atkinson Cycle Engine (DACE) with Heat Transfer Effects under Maximum Power and Maximum Power Density Conditions, *Applied Mathematical Modelling, 40* (2016), 13-14, pp. 6725-6736
[21] Dorić, Z. J., Klinar, J. I., Efficiency of a New Internal Combustion Engine Concept with Variable Piston Motion, *Thermal Science, 18* (2014), 1, pp. 113-127
[22] Horlock, J. H., Winterbone, D. E., *Thermodynamics and Gas Dynamics of Internal Combustion Engine*, Oxford University Press, Oxford, UK, 1986
[23] Lounici, M. S., *et al*., Investigation on Heat Transfer Evaluation for a More Efficient Two-Zone Combustion Model in the Case of Natural Gas SI engines, *Applied Thermal Engineering, 31* (2010), 2-3, pp. 319-328
[24] Curto-Risso, *et al*., Optimizing the Geometrical Parameters of a Spark Ignition Engine: Simulation and Theoretical Tools*, Applied Thermal Engineering, 31* (2011), 5, pp. 803-810
[25] Pourkhesalian, A. M., *et al*., Alternative Fuel and Gasoline in an SI Engine: A Comparative Study of Performance and Emissions Characteristics, *Fuel, 89* (2010), 5, pp. 1056-1063
[26] Mehrnoosh, D., *et al*., Thermodynamic model for prediction of performance and emission characteristics of SI engine fuelled by gasoline and natural gas with experimental verification, *Journal of Mechanical Science and Technology, 26* (2012), 7, pp. 2213-2225
[27] Tirkey, J. V., *et al*., Thermodynamic Integrated Gas Gynamic and Thermodynamic Computational Modeling of Four Stroke SI Engine Using Gasoline as a Fuel, *Thermal Science*, *13* (2009), 3, pp. 113-130
[28] Klimov, A. M., Premixed Turbulent Flame – Interplay of Hydrodynamic and Chemical Phenomena, *Americal institute of Astronautics and Aeronautics, 88* (1983), Jan., pp.133-146
[29] Gill, P. W., *et al., Fundamental of Internal Combustion Engine*, 4th Edition, Oxford & IBH Publishing Co. Pvt. Ltd, Inc., New Delhi, 1967

Paper submitted: May 20, 2017
Paper revised: November 13, 2017
Paper accepted: December 4-, 2017